DISTRACTED DRIVING DETECTION USING ON-BOARD SENSORS

Shigenobu Saigusa
Honda R&D Americas, Inc.
United States of America

Paper Number 19-0148

ABSTRACT

The frequency of distracted driving and its impact on safety is rapidly become a serious social issue. Given that distracted drivers pose an increased crash risk not only to themselves, but also to other road users, it is important to investigate ways to address this growing issue. This research project aims to realize a real-time identification and detection system for distracted driving for use in real-world driving scenarios. Therefore, the main goal of this research is development of a real-time model using on-board sensors, to classify whether the driver of the leading vehicle is distracted or not. This research also investigates the typical types of distracted driving behavior that can be detected by host vehicles (depending on the available sensors) and their key characteristics on driving data pattern.

INTRODUCTION

Safe driving requires drivers' continuous attention on the roadways. Any activities that compete for the driver's attention while driving have the potential to degrade driving performance and can lead to serious consequences for driving safety (Bao et al. 2015; Klauer et al. 2006; Sussman et al. 1985). According to NHTSA data, 3,179 people were killed in crashes that involved distracted driving on the U.S. roadways, which accounts for 10% of all fatalities in 2014 (NHTSA 2015). In addition, 431,000 people were injured in crashes that involved distracted driving, which accounts for 18% of all injuries (NHTSA 2015). The NHTSA report (NHTSA 2015) also indicated that the percentage of fatal and injury crashes due to cell phone use continuously increased over the most recent 5 years, whereas the total number of distraction-affected fatal and injury crashes stayed relatively stable. For example, 2,843 fatal crashes associated with distraction occurred in 2010, among which the percentage of related cell phone use was 12%, whereas in 2013, the total number of distraction-affected fatal crashes was 2,910, and the percentage of related cell phone use in distraction-affected fatal crashes increased to about 14%.

Distracted driving has been an increasing social concern. One of the challenging topics in distracted driving research is to identify and detect distracted driving from surrounding vehicles in a real-world driving setting. With the rapid development of in-vehicle based sensors (e.g., radar and camera), this issue has brought more attention to the transportation safety society including government, OEMs and suppliers. Previous efforts led by Honda have been conducted to develop algorithms to detect and predict lead vehicle's driver states using data from host vehicle sensors (Figure 1). The objective of this study focuses on modifying and prototyping the online detection algorithms to identify distracted driving behaviors on straight road driving. We also developed a prototype system as a pilot test of online detection algorithms.

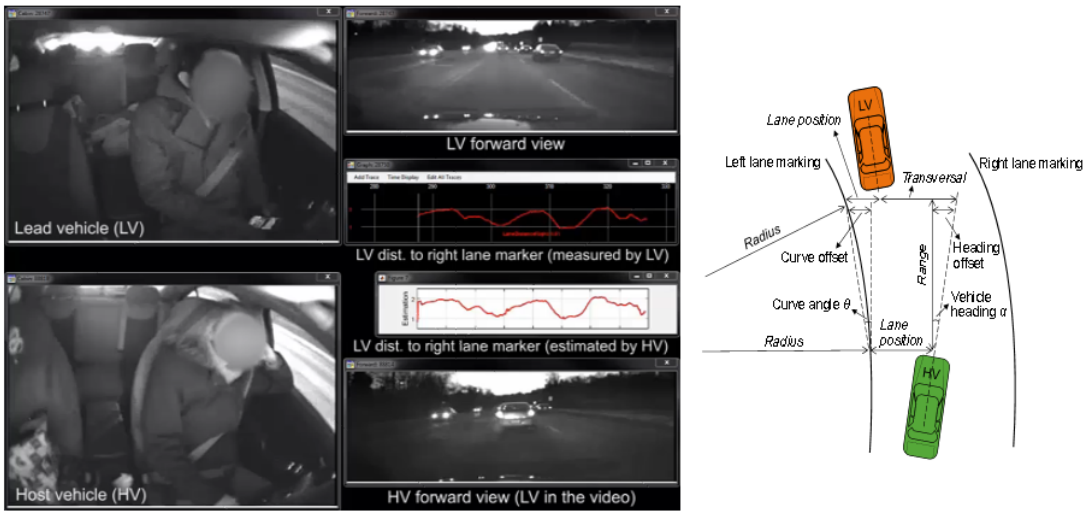

Figure 1. Lead vehicle distraction detection

LITERATURE REVIEW

In this section, a literature search and review was conducted to identify driver behavior models and parameter settings.

- Comparison and evaluation of advanced motion models for vehicle tracking: Schubert, R., Richter, E., & Wanielik, G. (2008, June). Comparison and evaluation of advanced motion models for vehicle tracking. In *Information Fusion, 2008 11th International Conference on* (pp. 1-6). IEEE.
    - The paper introduces 6 tracking models: CV (constant velocity), CA (constant acceleration), CSAV (constant steering angle and velocity). CTRV (constant turn rate and velocity), CTRA (constant turn rate and acceleration), CCA (constant curvature and acceleration) and show their relationship. It discusses 3 model fitting methods: Linear Kalman Filter, Extended Kalman Filter and Unscented Kalman filter. The extended Kalman Filter is the first-order approximation when the transition equation is not linear and the unscented Kalman Filter is the second-order approximation when the transition equation is not linear. In our work, we applied CV, CA and CTRA model. The CV model does not perform well but the CA and CTRA model are useful to detect the distraction driving behaviors. To fit the CA and CTRA model, the Linear Kalman Filter and Extended Kalman Filter are used.
- Two novel metrics for determining the tuning parameters of the Kalman Filter: Saha, M., Goswami, B., & Ghosh, R. (2011). Two novel costs for determining the tuning parameters of the Kalman Filter. *arXiv preprint arXiv:1110.3895*.
    - The paper shows a new approach to determine Q matrix in Linear Kalman Filter and Extended Kalman Filter. It defines J1, J2 as two metrics for determining Q matrix and also defines nq. These parameters are used to tune the Q matrix in Kalman Filters. As nq changes, the values of both J1 and J2 change between these limits of the number of measurements and 0. A large J1 indicates a sensitivity in the RMSE performance but this might also cause the filter to diverge while a large J2 indicates that the filter exhibits robustness for those combinations of the tuning parameters. In our work, we tried the novel metrics but they did not contribute in detecting distraction behaviors. We also tried to minimize RMSE for each of the tracking models but it could not make a fair comparison between these models. As a result, we decided to model the Q matrix based on physical knowledge and then fixed the parameters as the empirical values.

- Unscented Kalman filter design for curvilinear motion models suitable for automotive safety application: Tsogas, M., Polychronopoulos, A., & Amditis, A. (2005, July). Unscented Kalman filter design for curvilinear motion models suitable for automotive safety applications. In *Information Fusion, 2005 8th International Conference on* (Vol. 2, pp. 8-pp). IEEE.
    - The paper derives CTRA model and compares Unscented Kalman Filter with Extended Kalman Filter based on RMSE. In our work, we prefer Extended Kalman Filter rather than Unscented Kalman Filter for simplification.
- A comparative study of multiple model algorithms for maneuvering target tracking: Pitre, R. R., Jilkov, V. P., & Li, X. R. (2005, March). A comparative study of multiple-model algorithms for maneuvering target tracking. In *Proc. SPIE* (Vol. 5809, pp. 549-560).
    - The paper shows 7 multiple model algorithms: AMM (autonomous multiple model), GPB1 (first-order generalized Pseudo-Bayesian), GPB2 (second-order generalized Pseudo-Bayesian), Interacting MM, Reweighted MM, B-Best MM, Viterbi MM. It also compares different algorithms in a target tracking application. In our work, *w*e used AMM model to integrate different tracking models in the Extended Kalman Filter framework.
- An integrated solution for lane level irregular driving detection on highways: Sun, R., Ochieng, W. Y., & Feng, S. (2015). An integrated solution for lane level irregular driving detection on highways. *Transportation Research Part C: Emerging Technologies*, *56*, 61-79.
    - This paper proposes an integrated solution for the lane level irregular driving detection. Access to high accuracy positioning is enabled by GNSS and Inertial Navigation System (INS) integration using filtering with precise vehicle motion models and lane information. The detection of different types of irregular driving behavior is based on the application of a Fuzzy Inference System (FIS). The evaluation of the designed integrated systems in the field test shows that 0.5 m accuracy positioning source is required for lane level irregular driving detection algorithm and the designed system can detect irregular driving styles. In our work, the method is developed for the real road driving data instead of the simulation data. Also, our method does not require strict definitions of distraction behaviors.

METHOD

Our previous works from last years has three parts, one was to identify factors that contribute to distraction detection, the second part was to develop algorithms estimating lead vehicle trajectories by using host vehicle sensors (Feng, Bao, et al., 2017), and the third part was developing the algorithms to detect distracted driving. Table 1 summarizes the detection results from last year.

Table1. Summary of the results from last year work

Dataset	# of Events	Total Mileage	Time threshold	Detection rate	False alarm	False alarm rate
IVBSS (training set)	17	35.26	+-10s	71%	3	1 per 11.75 miles
Safe Pilot (test set)	32	131.85	+-20s	66%	15	1 per 8.79 miles

As the prediction accuracy reached about 66%, there were several limitations from the work last year:

- The previous algorithm (part 3) did not combine with the estimation algorithm (part 2);
- The output of prediction was binary, distracted or not (no probability of distraction);

- The detection rate was not high even in the training dataset;
- Only one test dataset was used for validation.

Based on previous work, the goals of the work of this year are centered on improving detection accuracy (probability based) and combining the lead vehicle trajectory estimation algorithm and distraction detection algorithms. Three models are used in the distraction detection algorithm development, Constant Velocity (CV), Constant Acceleration (CA), and Constant Turn Rate and Acceleration (CTRA) Model. A multiple model algorithm is then developed by integrating the results from the three models to find the best results (Figure 2). The final decision is based on the results from the integrated algorithms.

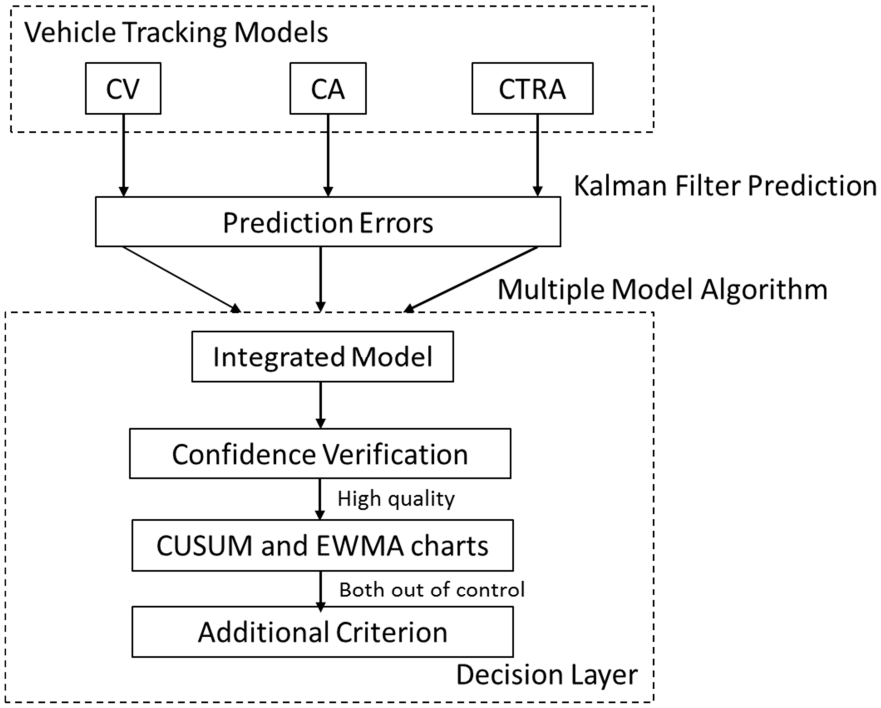

Figure 2. Flow chart of the distraction detection algorithm

KALMAN FILTER MODELING

Kalman Filter method was used to in all three models for the prediction purposes.

Vehicle tracking models

1. Constant Velocity model

We assume the vehicle speed is constant within each sampling interval $\Delta t = 0.1sec$ and use a four-dimensional state vector to formulate the transition equation as:

$$\begin{pmatrix} L_{x,k+1} \\ L_{y,k+1} \\ V_{x,k+1} \\ V_{y,k+1} \end{pmatrix} = \begin{pmatrix} 1 & 0 & \Delta t & 0 \\ 0 & 1 & 0 & \Delta t \\ 0 & 0 & 1 & 0 \\ 0 & 0 & 0 & 1 \end{pmatrix} \begin{pmatrix} L_{x,k} \\ L_{y,k} \\ V_{x,k} \\ V_{y,k} \end{pmatrix} + W = \begin{pmatrix} L_{x,k} + V_{x,k}\Delta t \\ L_{y,k} + V_{y,k}\Delta t \\ V_{x,t} \\ V_{y,t} \end{pmatrix} + W$$

.

where Lx, Ly, Vx and Vy denote longitudinal position, lateral position, longitudinal velocity and lateral velocity, respectively. The W is the process noise following a multivariate normal distribution with mean 0 and covariance matrix Q. The observed signal is denoted by Z, which is related to the state vector via:

$$Z_{k+1} = \begin{pmatrix} 0 & 0 & 1 & 0 \\ 0 & 1 & 0 & 0 \end{pmatrix} \begin{pmatrix} L_{x,k+1} \\ L_{y,k+1} \\ V_{x,k+1} \\ V_{y,k+1} \end{pmatrix} + U = \begin{pmatrix} V_{x,k+1} \\ L_{y,k+1} \end{pmatrix} + U$$

,

where U is the measurement error that follows a normal distribution with mean 0 and covariance matrix R. In other words, only longitudinal velocity and lateral position are observable.

2. Constant Acceleration model

We assume the vehicle acceleration is constant within each sampling interval. Therefore, we introduce 2 more dimensions to describe longitudinal (ax) and lateral accelerations (ay) besides the 4 dimensions in the CV model. The transition equation is written as:

$$\begin{pmatrix} L_{x,k+1} \\ L_{y,k+1} \\ V_{x,k+1} \\ V_{y,k+1} \\ a_{x,k+1} \\ a_{y,k+1} \end{pmatrix} = \begin{pmatrix} 1 & 0 & \Delta t & 0 & \frac{1}{2}\Delta t^2 & 0 \\ 0 & 1 & 0 & \Delta t & 0 & \frac{1}{2}\Delta t^2 \\ 0 & 0 & 1 & 0 & \Delta t & 0 \\ 0 & 0 & 0 & 1 & 0 & \Delta t \\ 0 & 0 & 0 & 0 & 1 & 0 \\ 0 & 0 & 0 & 0 & 0 & 1 \end{pmatrix} \begin{pmatrix} L_{x,k} \\ L_{y,k} \\ V_{x,k} \\ V_{y,k} \\ a_{x,k} \\ a_{y,k} \end{pmatrix} + W = \begin{pmatrix} L_{x,k} + V_{x,k}\Delta t + \frac{1}{2}a_{x,k}\Delta t^2 \\ L_{y,k} + V_{y,k}\Delta t + \frac{1}{2}a_{y,k}\Delta t^2 \\ V_{x,k} + a_{x,k}\Delta t \\ V_{y,k} + a_{y,k}\Delta t \\ a_{x,k} \\ a_{y,k} \end{pmatrix} + W$$

where W is the process noise. Longitudinal velocity and lateral position are the only observable signals, therefore the observation vector Z is written as:

$$Z_{k+1} = \begin{pmatrix} 0 & 0 & 1 & 0 & 0 & 0 \\ 0 & 1 & 0 & 0 & 0 & 0 \end{pmatrix} \begin{pmatrix} L_{x,k+1} \\ L_{y,k+1} \\ V_{x,k+1} \\ V_{y,k+1} \\ a_{x,k+1} \\ a_{y,k+1} \end{pmatrix} + U = \begin{pmatrix} V_{x,k+1} \\ L_{y,k+1} \end{pmatrix} + U$$

,

where U is the measurement error.

3. Constant Turn Rate and Acceleration model

This model can only be used for fitting straight road driving data because the road direction information is not available. The longitudinal acceleration and turn rate are assumed constant. The state vector is $\boldsymbol{x}_{t+1} = [x, y, \theta, v, \omega, a]^T$ representing longitudinal position, lateral position, and vehicle heading angle, longitudinal velocity, yaw rate and longitudinal acceleration, respectively. The transition equation is modelled by a transition function f:

$$\boldsymbol{x}_{t+1} = f(\boldsymbol{x}_t) + u, u \sim N(0, Q);$$

where u is the process noise. The transition function f is calculated according to the physical laws as:

$$
\begin{aligned}
x_{t+\Delta t} &= x_t + \frac{v_t}{\omega_t}(sin(\theta_t + \omega_t \Delta t) - sin(\theta_t)) + \frac{a_t \Delta t}{\omega_t} sin(\theta_t + \omega_t \Delta t) - \frac{a_t}{\omega_t^2} cos(\theta_t) + \frac{a_t}{\omega_t^2} cos(\theta_t + \omega_t \Delta t) \\
y_{t+\Delta t} &= y_t + \frac{v_t}{\omega_t}(cos(\theta_t) - cos(\theta_t + \omega_t \Delta t)) - \frac{a \Delta t}{\omega_t} cos(\theta_t + \omega_t \Delta t) + \frac{a_t}{\omega_t^2} sin(\theta_t + \omega_t \Delta t) - \frac{a_t}{\omega_t^2} sin(\theta_t) \\
\theta_{t+\Delta t} &= \theta_t + \omega_t \Delta t \\
v_{t+\Delta t} &= v_t + a_t \Delta t \\
\omega_{t+\Delta t} &= \omega_t \\
a_{t+\Delta t} &= a_t
\end{aligned}
,
$$

which is a nonlinear function of the state vector. The Extended Kalman Filter approximates the transition function f by using its Jacobian matrix J, where

$$
J = \begin{pmatrix}
1 & 0 & a_1 & a_2 & a_3 & a_4 \\
0 & 1 & a_5 & a_6 & a_7 & a_8 \\
0 & 0 & 1 & 0 & \Delta t & 0 \\
0 & 0 & 0 & 1 & 0 & \Delta t \\
0 & 0 & 0 & 0 & 1 & 0 \\
0 & 0 & 0 & 0 & 0 & 1
\end{pmatrix}
$$

and a's are partial derivative of f with respect to each dimension of the state vector x. This approximation yields $\boldsymbol{x}_{t+1} \approx J\boldsymbol{x}_t + u$. The longitudinal velocity, lateral position and yaw rate are observable on each sampling point. Therefore, we write the observation vector Z as:

$$
\boldsymbol{z}_{t+1} = H\boldsymbol{x}_{t+1} + r = \begin{pmatrix} y_{t+1} \\ v_{t+1} \\ \omega_{t+1} \end{pmatrix} + r, r \sim N(0, R).
$$

Here $H = \begin{pmatrix} 0 & 1 & 0 & 0 & 0 & 0 \\ 0 & 0 & 0 & 1 & 0 & 0 \\ 0 & 0 & 0 & 0 & 1 & 0 \end{pmatrix}$ and r denotes the measurement error.

4. Kalman Filter algorithm

Let X denote the state vector, F denote the transition matrix and Q denote the process noise. The objective of the Kalman Filter is to predict the distribution of X at time k with information from time 1 to k-1 and fit the distribution of X at time k given information from time 1 to k. In the prediction step, we have:

$$
\hat{X}_{k|k-1} = F\hat{X}_{k-1|k-1}
$$

and

$$
P_{k|k-1} = FP_{k-1|k-1}F^T + Q,
$$

Where $\hat{X}_{k|k-1}$ and $P_{k|k-1}$ denote the predicted mean and covariance at time k given information from time 1 to k-1, respectively. We then obtain the pre-fit residuals by comparing the predicted signals with observed signals:

$$
\tilde{Y}_k = Z_k - H\hat{X}_{k|k-1}
.
$$

The corresponding covariance matrix for the pre-fit residuals is calculated as:

$$
S_k = R + HP_{k|k-1}H^T
.
$$

We calculate the optimal Kalman gain and obtain the post-fit distributions by including the information of the observation at time k:

$$K_k = P_{k|k-1} H^T S_k^{-1},$$

$$\hat{X}_{k|k} = \hat{X}_{k|k-1} + K_k \tilde{Y}_k,$$

$$P_{k|k} = (I - K_k H) P_{k|k-1}.$$

The post-fit residual is calculated as $\tilde{y}_{k|k} = Z_k - H\hat{X}_{k|k}$ accordingly.

Kalman Filter parameters

1. R matrix for measurement error

The measurement errors of different signals are assumed independent of each other. The R matrix for different models are hence assumed diagonal matrix with each diagonal element representing the variance of measurement errors of the corresponding signals. In our model, we need to specify the variance of measurement errors of all observable signals, which are longitudinal velocity, lateral position and yaw rate. At the current stage, they take empirical values as 0.01, 0.45 and 0.1.

2. Q matrix for process noise

The process noise is the signal magnitude that is omitted in the transition model. The derivation requires the assumption that the acceleration and yaw rate are random variables within the sampling interval. Specifically, they are assumed to be follow a normal distribution with known mean and variance. In the CV model, we assume the longitudinal and lateral acceleration independently follow normal distribution with mean zero and variance $\sigma_{a,x}^2$ and $\sigma_{a,y}^2$. The Q matrix is derived by comparing CV model with the model with random accelerations, which is:

$$Q_{CV} = \begin{pmatrix} \frac{1}{4}\Delta t^4 \sigma_{a,x}^2 & 0 & \frac{1}{2}\Delta t^3 \sigma_{a,x}^2 & 0 \\ 0 & \frac{1}{4}\Delta t^4 \sigma_{a,y}^2 & 0 & \frac{1}{2}\Delta t^3 \sigma_{a,y}^2 \\ \frac{1}{2}\Delta t^3 \sigma_{a,x}^2 & 0 & \Delta t^2 \sigma_{a,x}^2 & 0 \\ 0 & \frac{1}{2}\Delta t^3 \sigma_{a,y}^2 & 0 & \Delta t^2 \sigma_{a,y}^2 \end{pmatrix}.$$

Similarly, we derive the Q matrix for CA and CTRA model as:

$$Q_{CA} = \begin{pmatrix} \frac{1}{4}\Delta t^4 \sigma_{a,x}^2 & 0 & \frac{1}{2}\Delta t^3 \sigma_{a,x}^2 & 0 & \frac{1}{2}\Delta t \sigma_{a,x}^3 & 0 \\ 0 & \frac{1}{4}\Delta t^4 \sigma_{a,y}^2 & 0 & \frac{1}{2}\Delta t^3 \sigma_{a,y}^2 & 0 & \frac{1}{2}\Delta t \sigma_{a,y}^3 \\ \frac{1}{2}\Delta t^3 \sigma_{a,x}^2 & 0 & \Delta t^2 \sigma_{a,x}^2 & 0 & \Delta t \sigma_{a,x}^2 & 0 \\ 0 & \frac{1}{2}\Delta t^3 \sigma_{a,y}^2 & 0 & \Delta t^2 \sigma_{a,y}^2 & 0 & \Delta t \sigma_{a,y}^2 \\ \frac{1}{2}\Delta t \sigma_{a,x}^3 & 0 & \Delta t \sigma_{a,x}^2 & 0 & \sigma_{a,x}^2 & 0 \\ 0 & \frac{1}{2}\Delta t \sigma_{a,y}^3 & 0 & \Delta t \sigma_{a,y}^2 & 0 & \sigma_{a,y}^2 \end{pmatrix},$$

$$Q_{CTRV} = G \begin{pmatrix} \sigma_a^2 & 0 \\ 0 & \sigma_\omega^2 \end{pmatrix} G^T,$$

$$G = \begin{pmatrix} a_4 & a_3 \\ a_8 & a_7 \\ 0 & \Delta t \\ \Delta t & 0 \\ 0 & 1 \\ 1 & 0 \end{pmatrix}$$

These Q matrices are determined by the standard deviation of longitudinal acceleration, lateral acceleration and yaw rate. Those values are pre-specified based on empirical knowledge, which are 0.3, 0.1 and 0.1, respectively.

Multiple model algorithm

The purpose of using multiple model algorithm is to switch between different tracking models to guarantee the tracking accuracy. The distraction behaviors are detected when none of the models provides an acceptable tracking accuracy. We integrate multiple models based on the residual likelihood. Because the pre-fit residual in a Kalman Filter follow normal distribution with mean 0 and known covariance matrix $S_k^{(i)}$. The likelihood is calculated as the density of the multivariate normal distribution:

$$L_k^{(i)} = f(\tilde{Y}_k^{(i)})$$
$$\tilde{Y}_k^{(i)} = Z_k^{(i)} - H\hat{X}_{k|k-1}^{(i)}$$
$$S_k^{(i)} = HP_k^{(i)}H^T + R \quad ,$$

where i represents the model index (i=1: CV, i=2: CA, i=3: CTRA). Normalizing the likelihood yields weight coefficients for each of the tracking model:

$$w_k^{(i)} = \frac{L_k^{(i)}}{\sum_{j=1}^{3} L_k^{(j)}} \quad .$$

The overall post-fit state vector is then calculated as the weighted average of the post-fit state vector of each of the tracking models as:

$$\hat{X}_{k|k} = \sum_{i=1}^{3} w_k^{(i)} \hat{X}_{k|k}^{(i)} \quad .$$

Control chart methods

1. CUSUM chart for prediction error monitoring

Signal patterns during abnormal driving periods cannot be well explained by the known physical models. We would like to relate the abnormal driving periods with high prediction errors from the fused vehicle tracking models obtained from the multiple model algorithm. Consequently, monitoring the variance of the prediction errors using CUSUM control chart helps detect the distraction behaviors. To calculate the variance, we set the window size as 10, which is to make decision for each consecutive 10-time points. The monitoring statistics are calculated as below:

$$v_i = \frac{\sqrt{|(\tilde{Y}_i - \mu_0)/\sigma|} - 0.822}{0.349} \sim N(0,1)$$
$$\bar{v}_i = \frac{1}{\sqrt{10}} \sum_{t=i+1}^{i+10} v_t \sim N(0,1)$$
$$S_i^+ = \max\{0, \bar{v}_i - k + S_{i-1}^+\}$$
$$S_i^- = \max\{0, -\bar{v}_i - k + S_{i-1}^-\}$$

Here, we set k = 0.5. According to the CUSUM control chart method, a time window is detected whenever the value S_i^+ is greater than the threshold H = 5.

2. EWMA chart for lane offset monitoring

Besides monitoring the error variance, we suggest monitoring the mean shift of lane offset signal at the same time. The lane-offset data is not normally distributed. EWMA control chart is recommended because it is less sensitive to the normality of the data. The monitoring statistic and the control limits are calculated as follows. Similar as CUSUM chart, the decision is made for each 10-time points. A time window is detected whenever the value Z_i is smaller than LCL_i or it is greater than UCL_i.

$$X_i: \text{ lane offset signal}$$

$$Z_0 = \bar{X}_{1:n}, n = 10$$

$$Z_i = \lambda \bar{X}_{(n-1)i+1:ni} + (1-\lambda) Z_{i-1}$$

$$\lambda = 0.2,\ L = 3$$

$$CL_i = 0$$

$$UCL_i = L\sigma\sqrt{\frac{\lambda}{2-\lambda}[1-(1-\lambda)^{2i}]}$$

$$LCL_i = -L\sigma\sqrt{\frac{\lambda}{2-\lambda}[1-(1-\lambda)^{2i}]}$$

Detection decision:

1. Combine CUSUM chart and EWMA chart

CUSUM chart monitors the variance of the prediction errors. It detects the time windows when the driving pattern is not predictable by the fused vehicle-tracking model. False alarms are generated if only CUSUM chart is used and the vehicle is waving around the center lane. EWMA chart monitors the mean shift of the lane-offset signal. It detects the time windows when the vehicle is off the center of the lane. False alarms are triggered if only EWMA chart is used and the driver has a habit of driving close to one of the lane edges. Therefore, we detect a time window if and only if the monitoring statistics are out of the control limits in both the control charts.

2. Evaluate distraction severity

We evaluate the distraction severity using distraction levels defined as below:

- Level = 0.5: EWMA chart generates alarms
- Level = 0.6: CUSUM chart generates alarms
- Level = 0.7: Both the charts generate alarms
- Level = 0.8: Both the charts generate alarms in consecutive two points (2 seconds)
- Level = 0.9: Both the charts generate alarms in consecutive three points (3 seconds)

We generate a distraction alarm for a time window when its distraction severity level is labeled as 0.9. To avoid the circumstances when the algorithm keeps generating alarms, we reset the monitoring statistics to zero in the next time window if a distraction alarm is triggered.

3. Mute the algorithm in special cases

The algorithm is designed for detecting the distraction behaviors during straight road driving only. It is muted in the following cases.

- Lane change: Lane change behaviors give rise to non-continuous lane offset signal patterns, which trigger false alarms. The algorithm is muted whenever a lane change behavior is detected.

- Curve driving: CTRA model cannot track the vehicle when it is in curves unless the vehicle's heading signal is given. When the vehicle's heading signal is not available, we have to assume the vehicle heading is as same as the lane heading, which implies that the algorithm only performs well during straight road driving periods. We mute the algorithm when the lane radius is smaller than 0.00015 meter.
- Low signal quality: the algorithm does not work when the signal measurements or estimation are not reliable. A frequent seen circumstance is that the lane boundary cannot be captured by camera.

RESULTS

When combining the leading vehicle estimation algorithm with the online detection algorithm, we only need to replace the measured signals Z as the estimated signals and change the corresponding observation errors to the estimation errors. The standard deviation of the estimation errors are estimated from the straight road driving segments when the leading vehicle is paired with the host vehicle. It is calculated as the sample variance of the differences between the estimated signals and the measured signals. Table 2. Summaries the detection results from different datasets. A relative high accuracy detection rate was observed.

Table 2. Prediction results summary

#	Dataset	Distracted	Curvature	Lane Change	Paired	Detection	False Alarm	Time between alarm (min)
1	IVBSS	No	Yes	No	No	NA	0/692s	NA
2	IVBSS	Yes	No	Yes	No	6/7	3/470s	2.6
3	IVBSS	No	Yes	Yes	No	NA	47/3880s	1.4
4	Safe Pilot	Yes	Yes	Yes	Yes	4/6	20/2924s	2.4
5	Safe Pilot	No	No	No	No	NA	0/762s	NA

Distracted: whether cell phone uses are observed in the video.

Curvature: whether curvy road segments are included during the trip.

Lane change: whether lane change behaviors are observed during the trip.

Paired: whether a host vehicle and a leading vehicle are paired to test the estimation algorithm.

Detection: detection rate (# of detections / # of total distraction behaviors).

False alarm: false alarm rate (# of false alarms / total driving time in second)

1. IVBSS Training Dataset

Description: This dataset is used to estimate the parameters in the Kalman Filter. No distracted behaviors are included during the trips.

- Parameters: (Trained in IVBSS Training Dataset)
- Standard deviation of observation error of Velocity: 0.45 m/s
- Standard deviation of observation error of Lane Offset: 0.01 m
- Standard deviation of observation error of Yaw Rate: 0.1 degree/s
- Standard deviation of longitudinal acceleration during cruise control: 0.3 m/s2

- Standard deviation of lateral acceleration during cruise control: 0.1 m/s2
- Standard deviation of angle acceleration during straight road driving: 0.1 degree/s2
- Standard deviation of prediction error of Lane Offset from Kalman Filter: 0.0523 m

2. IVBSS Distracted Driving Dataset

Description: Seven events are included in the dataset, each of which has a distraction period. The objective is to detect the distraction behavior during the period.

Parameters: (Trained in IVBSS Training Dataset) Same as 1

3. IVBSS Baseline Driving Dataset for Evaluating the False Alarm Rate (column 8 in the table)

Description: It is used to test the false alarm rate of the purposed algorithm.

Parameters: (Trained in IVBSS Training Dataset) Same as 1

4. Safe Pilot Distracted and Paired Driving Dataset

Description: Both the estimation algorithm and the detection algorithm are tested in the dataset. The estimated signals trigger slightly more false alarms than the directly measured signals. The standard deviations of the estimation errors are estimated based on the driving segments when both the lane quality and estimation confidence are high. In addition, we do not have the estimated yaw rate signal and therefore use the measured signal instead.

Parameters: (Trained in IVBSS Training Dataset and Safe Pilot Paired Driving Dataset)

- Standard deviation of estimation error of Velocity: 0.41 m/s
- Standard deviation of estimation error of Lane Offset: 0.49 m
- Standard deviation of estimation error of Yaw Rate: 0.1 degree/s
- Others: Same as 1

5. Safe Pilot Baseline Driving Dataset for Evaluating the False Alarm Rate (column 8 in the table)

Description: The dataset is used to evaluate the false alarm rate of the detection algorithm. As a result, no false alarm is triggered.

Parameters: (Trained in IVBSS Training Dataset) Same as 1

Table 3. Result comparison between the old and new algorithms

Method	Straight road only?	Length of test events	Paired cases?	Detection Rate	False Alarm Rate
Old	No	Approximately 7032s	No	68%	18/7032s (exclude vehicle passing)
New	Yes	8036s	Yes	77%	70/8036s (include vehicle passing)

CONCLUSIONS

In this work, an integrated multiple models was developed and applied. Control charts were used in the online detection decision. Results showed that a higher prediction accuracy and higher false alarm rate were observed, when compared to the results from previous work (Table 3). Methods and results from this work have provide a promising way and framework to the distracted driving detection. One limitation of this work is that only straight road driving was considered. Future work should be conducted to include curve road driving and how to reduce the false alarm rate.

REFERENCES

[1] Bao S, Guo Z, Flannagan C, Sullivan J, Sayer JR, LeBlanc D. Distracted driving performance measures: spectral power analysis. *Transp Res Rec.* 2015;2518:68–72.

[2] Klauer SG, Dingus TA, Neale VL, Sudweeks JD, Ramsey DJ. The Impact of Driver Inattention on Near-Crash/Crash Risk: An Analysis Using the 100-CarNaturalisticDriving StudyData. Springfield,VA:Virginia Tech Transportation Institute; 2006. DOT HS 810 594.

[3] NHTSA. 2015. Driver Electronic Device Use in 2014. 2015.Washington, DC.DOT HS 812 197.

[4] Sussman ED, BishopH,Madnick B, Walter R. Driver inattention and highway safety. Transp Res Rec. 1985;1047:40–48.